Supplementary Information

for

Excited-State Intramolecular Proton-Transfer Reaction Demonstrating Anti-Kasha Behavior

Huan-Wei Tseng,[a,‡] Jiun-Yi Shen,[a,‡] Ting-Yi Kuo,[a] Ting-Syun Tu,[a] Yi-An Chen,[a] Alexander P. Demchenko[b,*] and Pi-Tai Chou[a,*]

[a] Department of Chemistry, National Taiwan University, Taipei, 10617 Taiwan
[b] Palladin Institute of Biochemistry, National Academy of Sciences of Ukraine, Kiev 01030, Ukraine

‡ These authors contributed equally to this work.

Contents

Experimental Details

Synthesis and Characterizations

All reactions were carried out in oven- or flame-dried glassware under a positive pressure of N_2. All reagents were purchased commercially and used without further purification. TLC was performed on Merck 5715 silica gel 60 F254 pre-coated plates. Flash column chromatography was carried out using silica gel from Merck (230-400 mesh). ^{1}H-NMR (7.24 ppm for residual $CHCl_3$ in the $CDCl_3$ solvent as internal standard) and ^{13}C-NMR (77.0 ppm for $CDCl_3$ as internal standard) spectra were recorded on a Varian Unity-400 MHz instrument. Chemical shifts (δ) are quoted in parts per million (ppm) and coupling constants (J) are reported in Hertz (Hz). MS data was obtained using a Shimadzu LCMS-IT-TOF Mass Spectrometer. Single-crystal X-ray diffraction data were acquired on a Bruker SMART CCD diffractometer using λ (Mo-Kα) radiation (λ = 0.71073 Å). The data collection was executed using the SMART program. Cell refinement and data reduction were carried out with the SAINT program. The structure was determined using the SHELXTL/PC program and refined using full-matrix least squares. All non-hydrogen atoms were refined anisotropically, whereas hydrogen atoms were placed at calculated positions and included in the final stage of refinements with fixed parameters.

3-HTC. A mixture of thiophene-2-carbaldehyde (1.12 g, 10 mmol), 2-hydroxyacetophenone (1.36 g, 10 mmol), and NaOH (1.20 g, 30 mmol) in MeOH (60 mL) was heated under reflux for 5 h. The reaction mixture was cooled to room temperature. $NaOH_{(aq)}$ (1.0 N, 30 mL) and then hydrogen peroxide (35%, 4.5 mL) were added. After stirring overnight, the mixture was poured into ice-water and extracted with dichloromethane. The organic layer was dried over $MgSO_4$, filtered and evaporated. The crude product was purified by recrystallization from CH_2Cl_2 and hexane to yield **3-HTC** as a yellow solid (1.46 g, 60%). ^{1}H NMR (400 MHz, $CDCl_3$): δ 8.22 (dd, *J* = 8.0, 1.2 Hz, 1H), 8.00 (dd, *J* = 4.0, 1.2 Hz, 1H), 7.70-7.65 (m, 1H), 7.60 (dd, *J* = 5.2, 1.2 Hz, 1H), 7.56 (d, *J* = 8.4 Hz, 1H), 7.41-7.37 (m, 1H), 7.24-7.21 (m, 1H), 6.93 (s, 1H). ^{13}C NMR (100 MHz, $CDCl_3$): δ 172.5, 155.0, 142.6, 136.3, 133.5, 132.9, 129.8, 129.7, 128.1, 125.4, 124.5, 121.0, 118.1. FAB MS (m/z): 245 $(M+H)^+$.

3-HTCA. A mixture of 5-(1,3-dioxolan-2-yl)thiophene-2-carbaldehyde (1.84 g, 10 mmol), 2-hydroxyacetophenone (1.36 g, 10 mmol), and NaOH (1.20 g, 30 mmol) in MeOH (60 mL) was heated under reflux for 5 h. The reaction mixture was cooled to room temperature. $NaOH_{(aq)}$ (1.0 N, 30 mL) and then hydrogen peroxide (35%, 4.5 mL) were added to the mixture for stirring overnight. The mixture was evaporated and adjusted to pH 5 using 1.0 N $HCl_{(aq)}$. After extraction with dichloromethane, the organic layer was dried over $MgSO_4$, filtered and evaporated. The crude product was purified by recrystallization from CH_2Cl_2 and hexane to yield **3-HTCA** as a yellow solid (1.11 g, 40%). ^{1}H NMR (400 MHz, $CDCl_3$): δ 9.99 (s, 1H), 8.23 (d, *J* = 7.6 Hz, 1H), 8.05 (d, *J* = 4.0 Hz, 1H), 7.83 (d, *J* = 4.0 Hz, 1H), 7.73 (t, *J* = 7.6 Hz, 1H), 7.57 (d, *J* = 8.4 Hz, 1H), 7.43 (t, *J* = 8.4 Hz, 1H). ^{13}C NMR (100 MHz, $CDCl_3$): δ 183.0, 172.7, 155.2, 145.4, 141.5, 140.5, 138.0, 136.1, 134.3, 129.3, 125.5, 124.9, 120.8, 118.2. FAB MS (m/z): 273 $(M+H)^+$.

3-HTC-DiCN. A mixture of **3-HTCA** (0.70 g, 2.5 mmol), malononitirile (0.83 g, 12.5 mmol), and a catalytic amount of piperidine in THF (30 mL) and MeOH (30mL) was stirred for 3 days. The solid was filtered and washed with CH_2Cl_2 and MeOH to yield **3-HTC-DiCN** as an orange solid (0.30 g, 38%). ^{1}H NMR (400 MHz, THF-d_8): δ 10.2 (s, 1H), 8.35 (s, 1H), 8.17 (dd, *J* = 8.0, 2.0 Hz, 1H), 8.07 (d, *J* = 4.0 Hz, 1H), 7.96 (d, *J* = 4.8 Hz, 1H), 7.77-7.73 (m, 1H), 7.65 (d, *J* = 8.0 Hz, 1H), 7.44-7.40 (d, *J* = 8.0 Hz, 1H). ^{13}C NMR (100 MHz, THF-d_8): δ 173.1, 156.0, 152.0, 144.0,141.3, 140.7, 139.0, 138.7, 134.7, 129.2, 126.1, 125.4, 123.0, 118.9, 114.9, 114.3, 79.0. FAB MS (m/z): 321 $(M+H)^+$. The orange-red crystals of **3-HTC-DiCN** were grown in a THF solution. The crystal structure is shown in Fig. S1 and the crystal data, bond lengths, and angles are listed in Table S1 and S2.

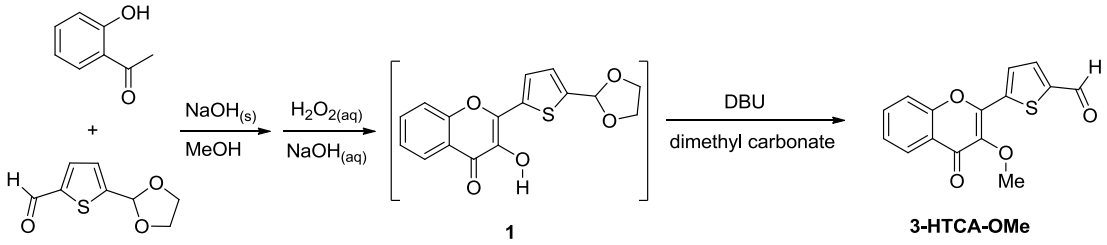

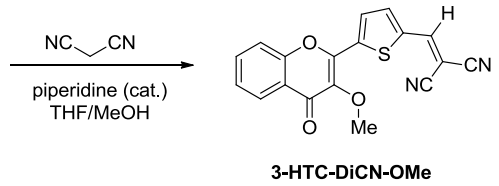

3-HTCA-OMe. A mixture of thiophene-2-carbaldehyde (0.56 g, 5.0 mmol), 2-hydroxyacetophenone (0.68 g, 5.0 mmol), and NaOH (0.60 g, 15 mmol) in MeOH (30 mL) was heated under reflux for 5 h. The reaction mixture was cooled to room temperature. $NaOH_{(aq)}$ (1.0 N, 15 mL) and then hydrogen peroxide (35%, 2.3 mL) were added. After stirring overnight, the mixture was poured into ice-water and extracted with dichloromethane. The organic layer was dried over $MgSO_4$, filtered and evaporated to form **1** and which was used in the next reaction without further purification. A mixture of **1** and DBU (1 mL) in dimethyl carbonate (40 mL) was heated under reflux for 2 days. The solvent was evaporated under reduced pressure. The residue was added into 1N HCl (50 mL) and extracted with ethyl acetate. The organic layer was dried over $MgSO_4$, filtered and evaporated. The crude product was purified by silica gel column chromatography with hexane/EtOAc mixture as eluent to afford **3-HTCA-OMe** as a light-yellow solid (0.78 g, 55%). ^{1}H NMR (400 MHz, $CDCl_3$): δ 10.03 (s, 1H), 8.25 (dd, *J* = 8.0, 1.6 Hz, 1H), 8.00 (d, *J* = 4.0, 1H), 7.83 (d, *J* = 4.4, 1H), 7.73-7.69 (m, 1H), 7.54 (d, *J* = 8.4 Hz, 1H), 7.44-7.40 (m, 1H), 4.15 (s, 3H). ^{13}C NMR (100 MHz, $CDCl_3$): δ 183.49, 174.02, 154.81, 149.52, 146.51, 140.55, 140.05, 135.27, 133.96, 129.30, 125.88, 125.03, 124.25, 117.85, 59.93. FAB MS (m/z): 287 $(M+H)^+$. Note that **3-HTCA-OMe** is not stable and a trace amount of impurity always exists

and is likely due to decomposition. The impurity makes it infeasible to perform reliable spectroscopy studies.

3-HTC-DiCN-OMe. A mixture of **3-HTCA-OMe** (0.50 g, 2.0 mmol), malononitirile (0.70 g, 10 mmol), and a catalytic amount of piperidine in THF (20 mL) and MeOH (20 mL) was heated under reflux overnight. The solvent was evaporated under reduced pressure and the residue was extracted with CH_2Cl_2. The organic layer was dried over $MgSO_4$, filtered and evaporated. The crude product was purified by column chromatography on silica gel with a CH_2Cl_2/EtOAc mixture as eluent to afford **3-HTC-DiCN-OMe** as a yellow solid (0.20 g, 30%). ^{1}H NMR (400 MHz, $CDCl_3$): δ 8.23 (dd, *J* = 8.0, 1.6 Hz, 1H), 8.00 (d, *J* = 4.0, 1H), 7.88 (d, *J* = 4.4, 1H), 7.84 (s, 1H), 7.73-7.68 (m, 1H), 7.54 (d, *J* = 8.4 Hz, 1H), 7.43-7.39 (m, 1H), 4.18 (s, 3H). ^{13}C NMR (100 MHz, $CDCl_3$): δ 154.79, 150.16, 140.87, 138.51, 136.81, 134.17, 129.63, 125.94, 125.20, 124.28, 117.89, 113.61, 112.94, 79.83, 60.14. FAB MS (m/z): 335 $(M+H)^+$.

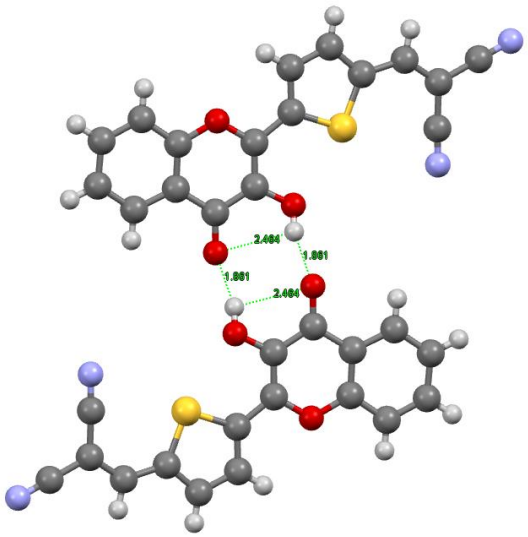

Fig. S1 The X-ray structure of the doubly hydrogen-bonded **3-HTC-DiCN** dimers in the crystalline state. (The distances of the intermolecular H-bonds (O-H···O=C) are both 1.861 Å while the intramolecular distances between the O2 atom and the H atom bounded to the O3 atom are both estimated to be 2.464 Å.)

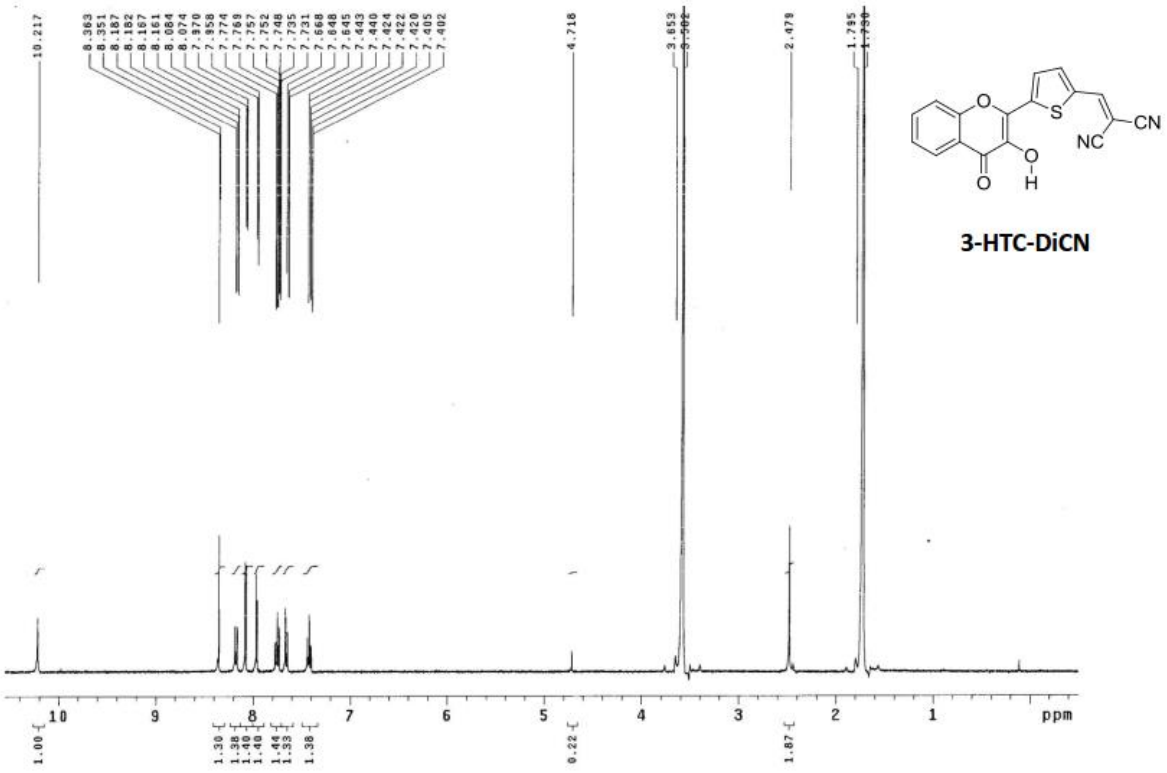

Fig. S2 The ^{1}H NMR spectroscopy of **3-HTC-DiCN** in THF-d_8.

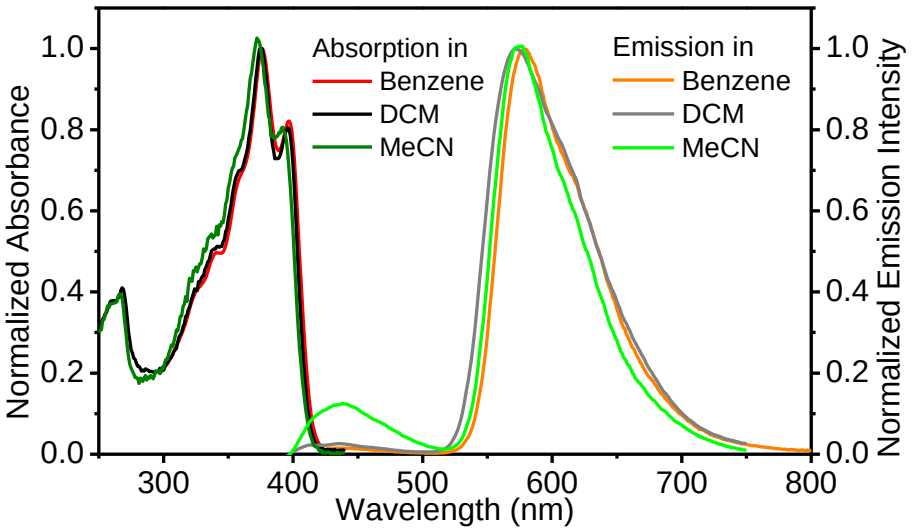

Fig. S3 Steady-state absorption and emission spectra (with 350 nm excitation) for **3-HTCA** in benzene, dichloromethane (DCM) and acetonitrile (MeCN). The low-intensity N* band appears in the emission spectrum on a very low level.

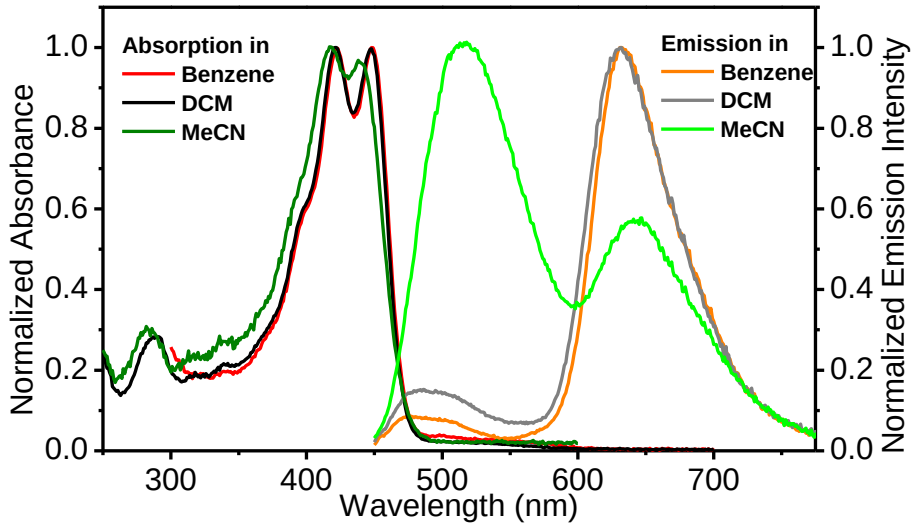

Fig. S4 Steady-state absorption and emission spectra (with 440 nm excitation) for **3-HTC-DiCN** in benzene, dichloromethane (DCM) and acetonitrile (MeCN). The presence of N* band in emission is clearly seen.

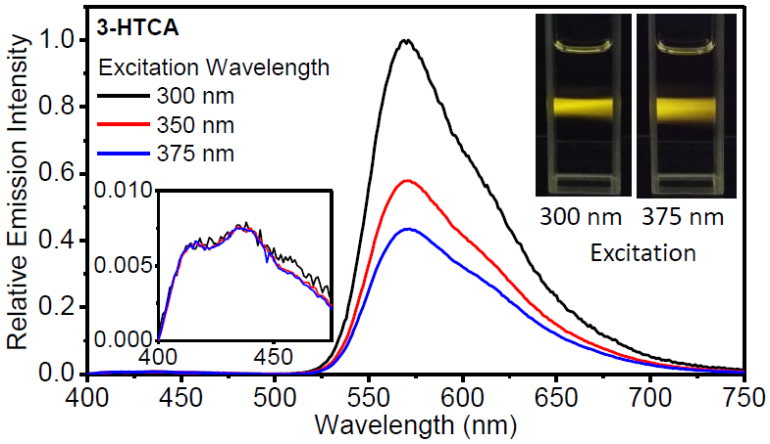

Fig. S5 Relative emission spectra for **3-HTCA** in CH_2Cl_2 with different excitation wavelengths. The emission intensities of the spectra are set to be the same at the peak of the normal form emission. Insets: photos of emission hue with a shorter- or a longer-wavelength excitation.

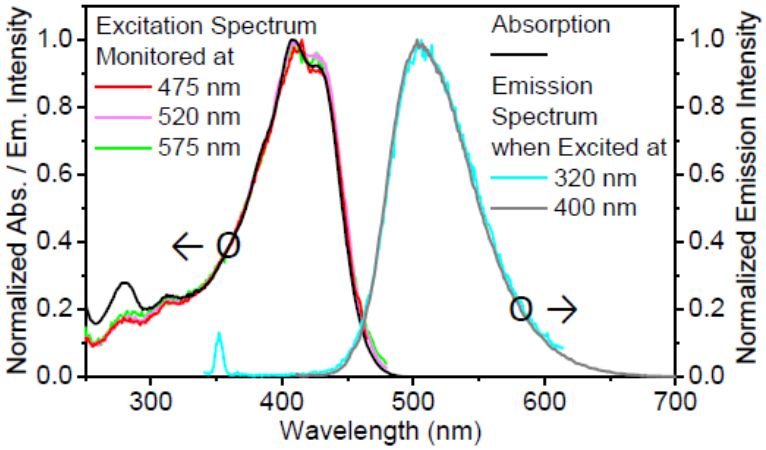

Fig. S6 Absorption, emission (excited at 320 nm and 400 nm) and excitation spectra (monitored at indicated wavelengths) for **3-HTC-DiCN-OMe** in CH_2Cl_2. All the excitation spectra are nearly identical to the absorption spectrum. The normalized emission spectra with 320 nm or 400 nm excitations are on top of each other. No extra emission bands (from higher energy states) can be observed with 320 nm excitation (note: the band peaked at 350 nm is due to Raman scattering). These results conclude no anti-Kasha behavior.

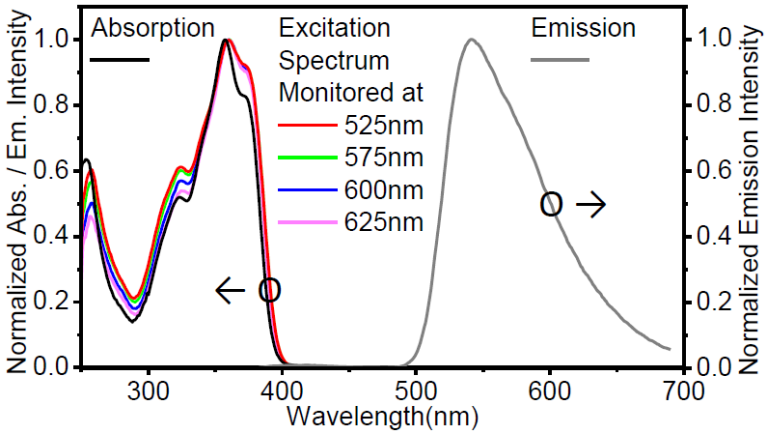

Fig. S7 Absorption, emission (excited at 350 nm) and excitation spectra (monitored at indicated wavelengths) for **3-HTC** in CH_2Cl_2. The results show only minor deviation from Kasha's rule.

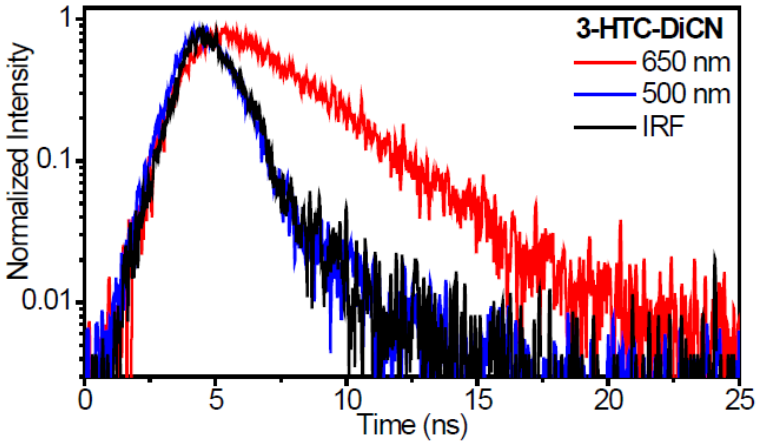

Fig. S8 Nanosecond time-resolved emission decays for **3-HTC-DiCN** recorded in CH_2Cl_2. The excitation wavelength is 400 nm. The emission kinetic traces of the N* form (blue) and the T* form (red) are recorded at indicated wavelengths. IRF (black) is the instrument responds function. As in the case of **3-HTC** the strong difference in long component of decays (For N* band it is almost unresolved from IRF) indicates the non-equilibrium character of ESIPT reaction.

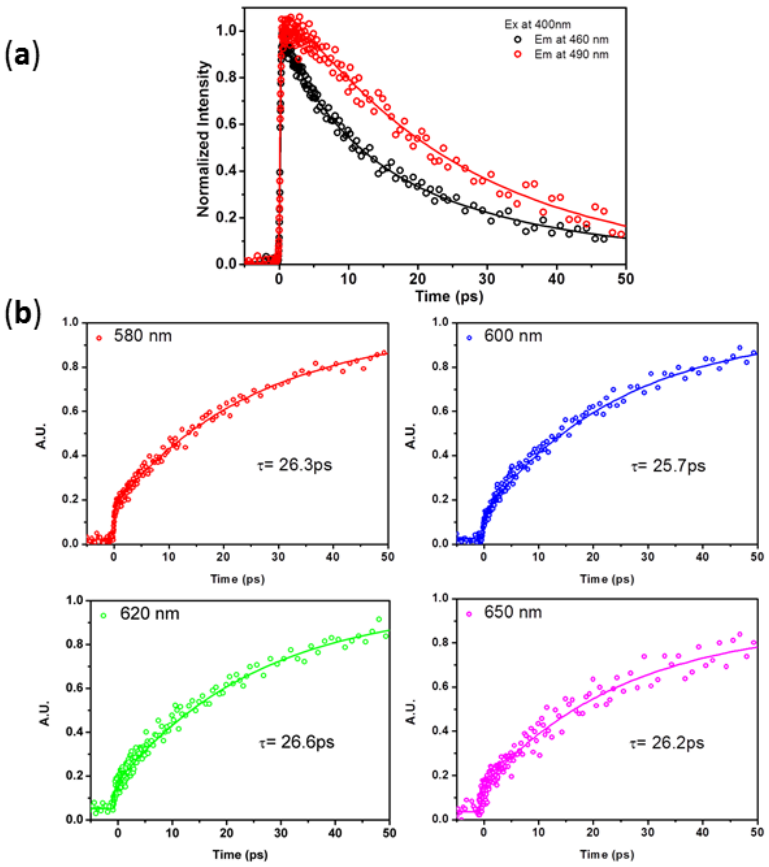

Fig. S9 Fluorescence up-conversion time-resolved kinetic traces for **3-HTCA** in CH_2Cl_2. (**a**) Upon 400 nm excitation, the dynamics of relaxation of the normal emission acquired at different wavelengths. (**b**) Excited-state tautomer (T*) emission kinetics is recorded at indicated wavelength with a 400 nm excitation. The presence of system response limited component at short wavelength edge of T* emission is due to ESIPT prior to solvent relaxtion.[29,30]

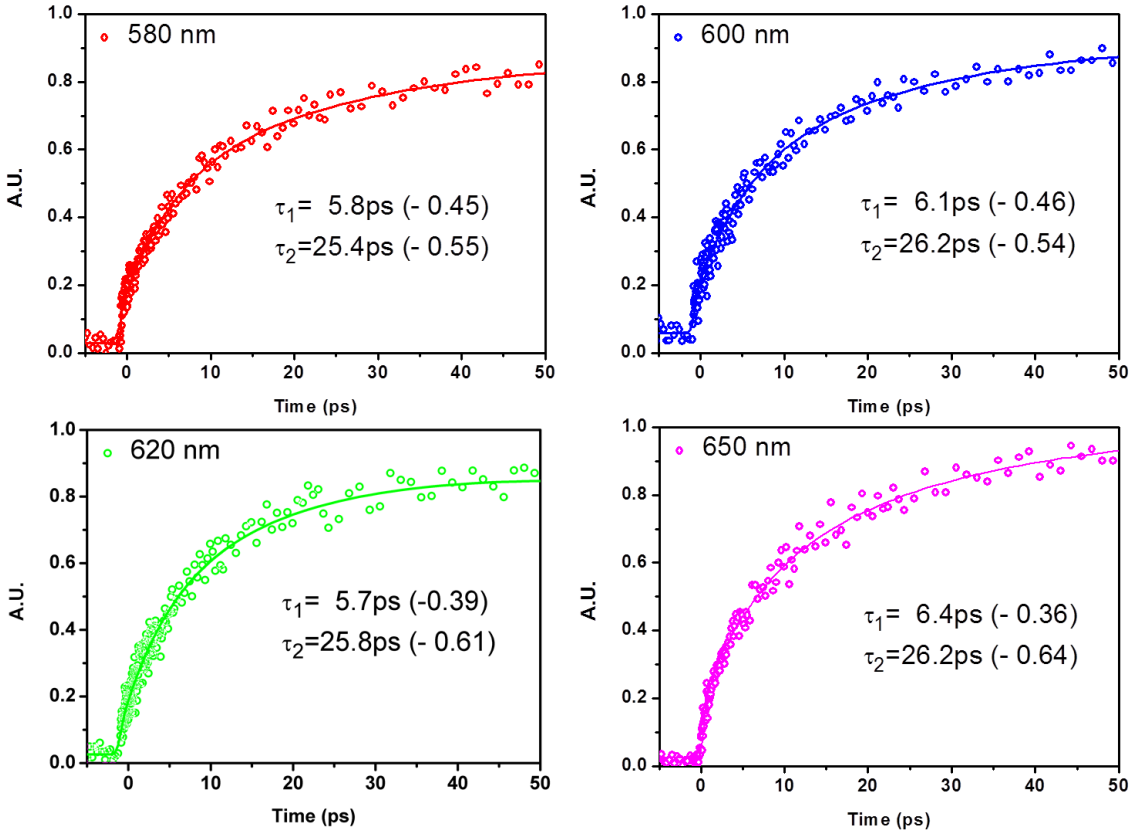

Fig. S10 Fluorescence up-conversion time-resolved kinetic traces for **3-HTCA** in CH_2Cl_2. Excited-state tautomer (T*) emission kinetics is recorded at indicated wavelength with a 350 nm excitation.

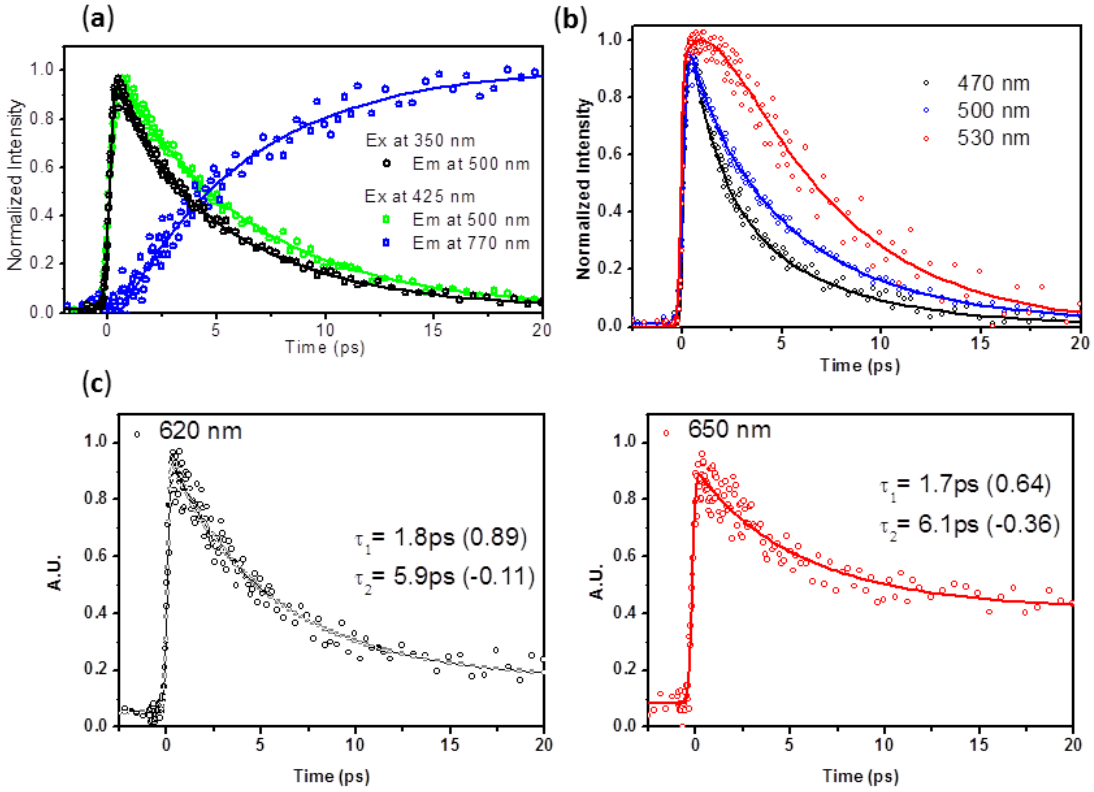

Fig. S11 Fluorescence up-conversion time-resolved kinetic traces for **3-HTC-DiCN** in CH_2Cl_2. (**a**) A comparison of emission decays and rises at indicated excitation and emission wavelengths. (**b**) Upon 350 nm excitation, the dynamics of relaxation of the normal emission acquired at several different wavelengths. (**c**) Emission kinetics recorded at indicated wavelengths for the T* emission with a 350 nm excitation.

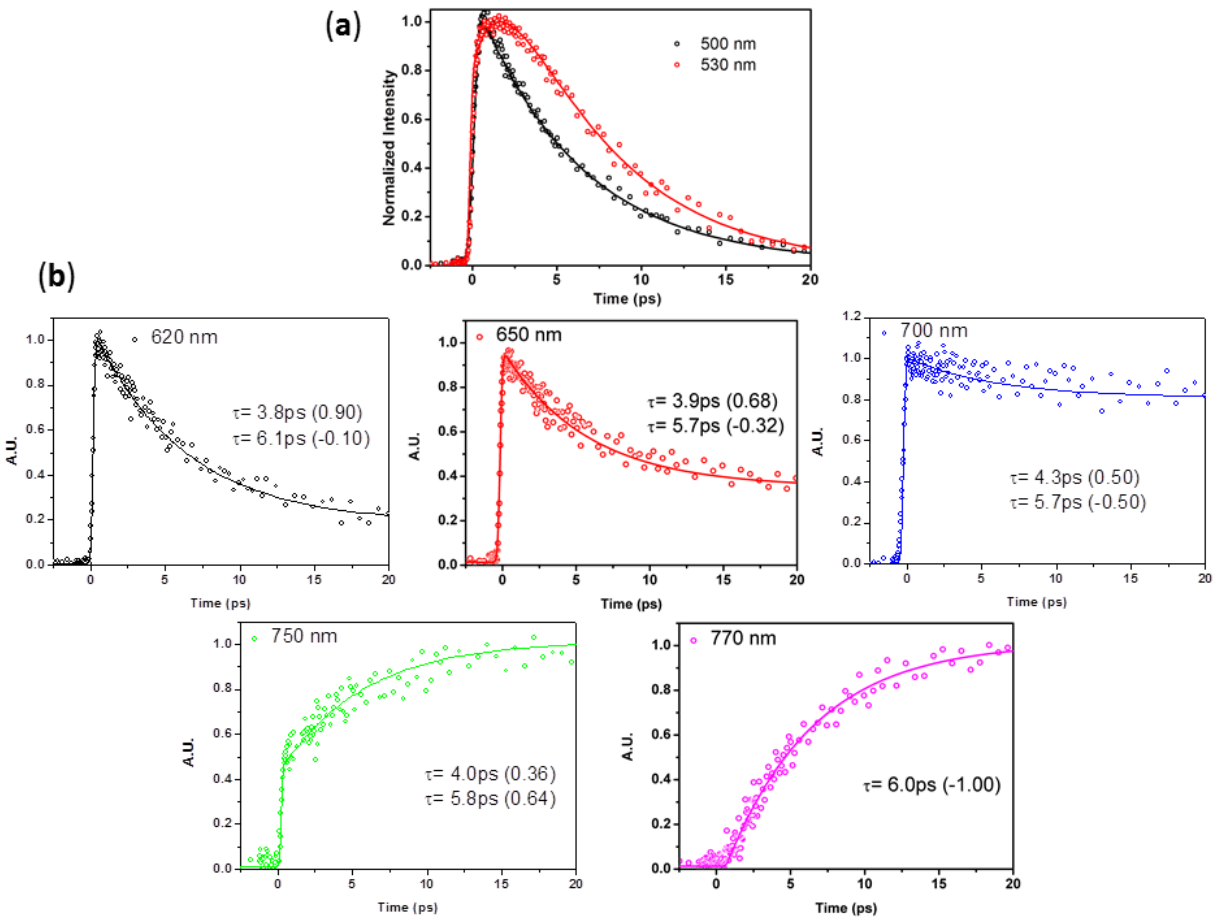

Fig. S12 Fluorescence up-conversion time-resolved kinetic traces for **3-HTC-DiCN** in CH_2Cl_2. (**a**) Upon 425 nm excitation, the dynamics of relaxation of the normal emission acquired at different wavelengths. (**b**) Emission kinetics recorded at indicated wavelengths for the T* emission with a 425 nm excitation.

Table S1 Single crystal data and structure refinements for **3-HTC-DiCN**

Identification code	ic15823
Empirical formula	C17 H8 N2 O3 S
Formula weight	320.31
Temperature	200(2) K
Wavelength	0.71073 Å
Crystal system	Monoclinic
Space group	P2(1)/c
Unit cell dimensions	a = 15.8828(18) Å b = 6.8328(8) Å c = 13.9502(16) Å α = 90° β =107.844(2)° γ = 90°
Volume	1441.1(3) $Å^3$
Z	4
Density (calculated)	1.476 Mg/m^3
Absorption coefficient	0.241 mm^{-1}
F(000)	656
Crystal size	0.32 x 0.30 x 0.02 mm^3
Theta range for data collection	1.35 to 25.00°
Index ranges	$-18 \leq h \leq 18$, $-8 \leq k \leq 8$, $-16 \leq l \leq 16$
Reflections collected	8334
Independent reflections	2537 [R(int) = 0.1061]
Completeness to theta = 25.00°	99.7 %
Absorption correction	Semi-empirical from equivalents
Max. and min. transmission	0.9952 and 0.9268
Refinement method	Full-matrix least-squares on F^2
Data / restraints / parameters	2537 / 0 / 209
Goodness-of-fit on F^2	1.090
Final R indices [I>2sigma(I)]	R1 = 0.0669, wR2 = 0.1620
R indices (all data)	R1 = 0.1021, wR2 = 0.2021
Largest diff. peak and hole	0.397 and -0.493 $e.Å^{-3}$

Table S2 Bond lengths and angles in the crystal structure of **3-HTC-DiCN**

Bond Lengths (Å)			
S(1)-C(10)	1.724(4)	C(5)-C(6)	1.412(5)
S(1)-C(13)	1.736(4)	C(6)-C(7)	1.444(5)
O(1)-C(9)	1.360(5)	C(7)-C(8)	1.432(6)
O(1)-C(1)	1.369(5)	C(8)-C(9)	1.363(5)
O(2)-C(7)	1.253(4)	C(9)-C(10)	1.451(6)
O(3)-C(8)	1.352(4)	C(10)-C(11)	1.383(5)
N(1)-C(16)	1.132(6)	C(11)-C(12)	1.377(6)
N(2)-C(17)	1.140(6)	C(12)-C(13)	1.380(6)
C(1)-C(2)	1.382(5)	C(13)-C(14)	1.423(6)
C(1)-C(6)	1.397(5)	C(14)-C(15)	1.349(6)
C(2)-C(3)	1.380(6)	C(15)-C(16)	1.430(7)
C(3)-C(4)	1.390(6)	C(15)-C(17)	1.446(6)
C(4)-C(5)	1.372(6)		
Bond Angles (°)			
C(10)-S(1)-C(13)	90.86(19)	C(9)-O(1)-C(1)	119.6(3)
O(1)-C(1)-C(2)	115.9(4)	O(1)-C(1)-C(6)	121.4(3)
C(2)-C(1)-C(6)	122.7(4)	C(3)-C(2)-C(1)	117.8(4)
C(2)-C(3)-C(4)	121.4(4)	C(5)-C(4)-C(3)	120.2(4)
C(4)-C(5)-C(6)	120.2(4)	C(1)-C(6)-C(5)	117.6(4)
C(1)-C(6)-C(7)	119.9(4)	C(5)-C(6)-C(7)	122.5(4)
O(2)-C(7)-C(8)	120.9(4)	O(2)-C(7)-C(6)	123.4(4)
C(8)-C(7)-C(6)	115.6(3)	O(3)-C(8)-C(9)	118.0(4)
O(3)-C(8)-C(7)	120.6(3)	C(12)-C(13)-C(14)	124.2(4)
C(9)-C(8)-C(7)	121.3(4)	C(12)-C(13)-S(1)	110.9(3)
O(1)-C(9)-C(8)	122.1(4)	C(14)-C(13)-S(1)	124.9(3)
O(1)-C(9)-C(10)	111.1(3)	C(15)-C(14)-C(13)	131.0(4)
C(8)-C(9)-C(10)	126.7(4)	C(14)-C(15)-C(16)	119.6(4)
C(11)-C(10)-C(9)	125.3(4)	C(14)-C(15)-C(17)	124.3(4)
C(11)-C(10)-S(1)	111.8(3)	C(16)-C(15)-C(17)	116.1(4)
C(9)-C(10)-S(1)	122.9(3)	N(1)-C(16)-C(15)	179.9(7)
C(12)-C(11)-C(10)	112.6(4)	N(2)-C(17)-C(15)	177.5(5)
C(11)-C(12)-C(13)	113.8(4)		

Table S3 Emission rise and decay lifetimes in the fs-ps time range for **3-HTCA** in CH_2Cl_2 with different excitation wavelengths (λ_{ex}) and monitored at various emission wavelengths (λ_{em})

compound	λ_{ex} (nm)	λ_{em} (nm)	τ_{obs} by uPL (ps)	pre-exponential factor
3-HTCA	350	430	3.8±0.3	0.41
			25.2±3.2	0.59
		460	4.6±0.7	0.29
			25.8±3.9	0.71
		490	2.8±0.2	-0.1
			4.3±0.5	0.2
			25.5±2.8	0.7
		580	5.8±0.7	−0.45 [a]
			25.4±3.0	−0.55 [a]
		600	6.1±0.6	−0.46 [a]
			26.2±2.6	−0.54 [a]
		620	5.7±0.7	−0.39 [a]
			25.8±3.4	−0.61 [a]
		650	6.4±0.8	−0.36 [a]
			26.2±3.1	−0.64 [a]
	400	460	25.4±3.6	1.00
		490	2.4±0.1	-0.15
			25.2±3.4	0.83
		580	26.3±2.6	−1.00 [a]
		600	25.7±2.1	−1.00 [a]
		620	26.6±3.5	−1.00 [a]
		650	26.2±3.1	−1.00 [a]

[a] Rise kinetics.

Table S4 Emission rise and decay lifetimes in the fs-ps time range for **3-HTC-DiCN** in CH_2Cl_2 with different excitation wavelengths (λ_{ex}) and monitored at various emission wavelengths (λ_{em})

compound	λ_{ex} (nm)	λ_{em} (nm)	τ_{obs} by uPL (ps)	pre-exponential factor
3-HTC-DiCN	350	470	1.3±0.2	0.58
			5.6±0.8	0.42
		500	1.5±0.2	0.42
			5.8±0.6	0.58
		530	1.3±0.2	-0.4
			1.5±0.2	0.28
			6.1±0.7	0.32
		620	1.8±0.1	0.89
			5.9±0.4	−0.11 [a]
		650	1.7±0.2	0.64
			6.1±0.9	−0.36 [a]
	425	500	6.2±0.8	1.0
		530	1.8±0.2	-0.37
			6.4±0.8	0.63
		620	3.8±0.4	0.90
			6.1±0.6	−0.10 [a]
		650	3.9±0.5	0.68
			5.7±0.8	−0.32 [a]
		700	4.3±0.5	0.50
			5.7±0.7	−0.50 [a]
		750	4.0±0.4	0.36
			5.8±0.6	−0.64 [a]
		770	6.0±0.8	−1.00 [a]

[a] Rise kinetics.

Calculations and Discussions on the Proton Transfer Efficiencies from the Higher Energy States

The equations needed are:

$$\frac{I_{N(\beta)}}{I_{N(\alpha)}} = \frac{\beta}{\alpha}(1-y) \qquad (eq.1)$$

$$\frac{I_{T(\beta)}}{I_{T(\alpha)}} = \frac{I_{N(\beta)}}{I_{N(\alpha)}} + \frac{\beta y}{\alpha x} \qquad (eq.3)$$

3-HTC-DiCN - Data taken from the absorption and excitation spectra (Fig. 4 & 5):

Wavelength (nm)	Relative Absorbance	Relative Emission Intensity in the Excitation Spectrum Monitored at	
		Normal Form (500 nm)	Tautomer Form (625 nm)
300	0.20	0.14	1.12
350	0.21	0.19	0.67
450	0.98	0.99	0.62

Using the data obtained at 350 and 450 nm:

For 350 nm, β = 0.21

450 nm, α = 0.98

→ $\frac{\beta}{\alpha} = \frac{0.21}{0.98} = 0.214$

For 350 nm, $I_{N(\beta)}$ = 0.19 and $I_{T(\beta)}$ = 0.67

450 nm, $I_{N(\alpha)}$ = 0.99 and $I_{T(\alpha)}$ = 0.62

→ $\frac{I_{N(\beta)}}{I_{N(\alpha)}} = \frac{0.19}{0.99} = 0.192$ and $\frac{I_{T(\beta)}}{I_{T(\alpha)}} = \frac{0.67}{0.62} = 1.08$

Plug the values into eq. 1

→ $0.192 = 0.214(1-y)$ ➔ $y = 0.103 = 10.3\%$

Then by using eq. 2

→ $1.08 = 0.192 + 0.214 \times \frac{0.103}{x}$ ➔ $x = 0.025 = 2.5\%$

Using the data obtained at 300 and 450 nm:

For 300 nm, β = 0.20

450 nm, α = 0.98

→ $\frac{\beta}{\alpha} = \frac{0.20}{0.98} = 0.204$

For 300 nm, $I_{N(\beta)}$ = 0.14 and $I_{T(\beta)}$ = 1.12

450 nm, $I_{N(\alpha)}$ = 0.99 and $I_{T(\alpha)}$ = 0.62

→ $\frac{I_{N(\beta)}}{I_{N(\alpha)}} = \frac{0.14}{0.99} = 0.141$ and $\frac{I_{T(\beta)}}{I_{T(\alpha)}} = \frac{1.12}{0.62} = 1.81$

Plug the values into eq. 1

→ $0.141 = 0.204(1 - y)$ ➔ $y = 0.309 = 30.9\%$

Then by using eq. 2

→ $1.81 = 0.141 + 0.204 \times \frac{0.309}{x}$ ➔ $x = 0.038 = 3.8\%$

Now, Fig. 9 can be updated by adding the new information obtained for **3-NTC-DiCN**:

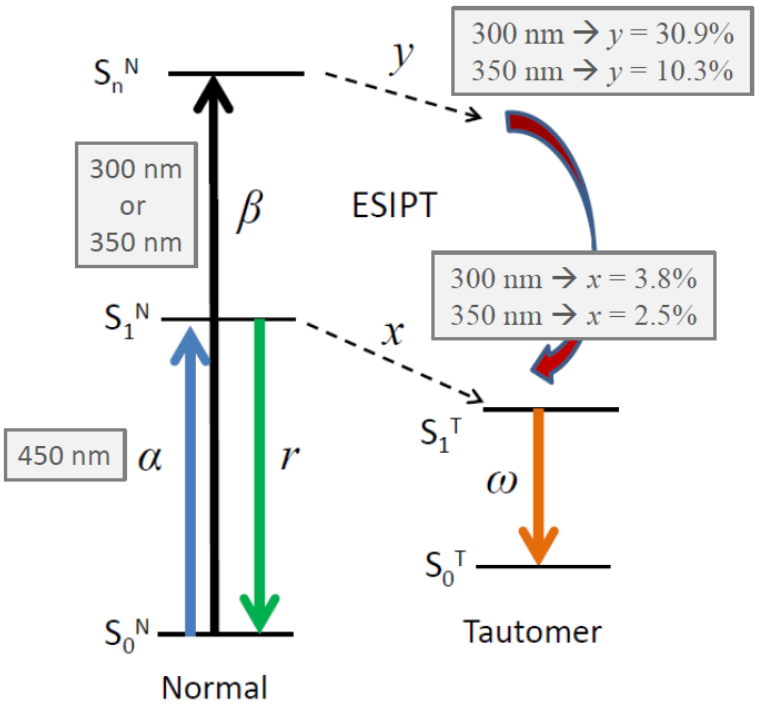

3-HTC-DiCN

The tautomer emission quantum yield (Φ_{em}) can be written as

$$\Phi_{em} = y\omega + (1-y)x\omega$$

From Table 1, when **3-HTC-DiCN** is excited at 300 nm, the tautomer emission quantum yield (Φ_{em}) is 0.060.

$$\rightarrow 0.060 = 30.9\% \times \omega + (1 - 30.9\%) \times 3.8\% \times \omega$$

$$\rightarrow \omega = 0.18$$

The emission quantum efficiency is low, which also explains why the excited-state tautomer lifetime is as long as 2.1 ns, but Φ_{em} is only 0.060.

Check point:

When **3-HTC-DiCN** is excited at 350 nm, the tautomer emission quantum yield can be estimated using the equation and the ω value obtained above:

$$\Phi_{em} = y\omega + (1-y)x\omega$$

$$\rightarrow \Phi_{em} = 10.3\% \times 0.18 + (1 - 10.3\%) \times 2.5\% \times 0.18$$

$$= 0.023$$

From Table 1, when **3-HTC-DiCN** is excited at 350 nm, the tautomer emission quantum yield (Φ_{em}) is 0.030 which is not far off from the estimated value.

Furthermore, the observed decay lifetime of the normal form emission of **3-HTC-DiCN** is about 6 ps, which corresponds to a k_{obs} of 1.67 x 10^{11} s^{-1}. Then the ESIPT rate from the S_1^N state can be calculated:

$$1.67 \times 10^{11}\ s^{-1} \times 3.15\%$$

$$= 5.26 \times 10^{9}\ s^{-1}$$

$$= 190\ ps$$

This is a much slower rate when compared with regular ESIPT (~1 ps). This result also indicates that proton-coupled charge transfer and solvent-induced barrier have channeled into the reaction coordinate (See Fig. 8).

When it brings to the resonance form, ESIPT is ultrafast. Also, given a fast solvent relaxation time constant of 1 ps in CH_2Cl_2,

$5.26 \times 10^9 s^{-1} = Ae^{-\Delta E/RT}$

→ $5.26 \times 10^9 s^{-1} = 1 \times 10^{12} s^{-1} \times e^{-\Delta E/RT}$

→ $e^{-\Delta E/RT} = 0.00526$

→ $-\Delta E/RT = ln\, 0.00526$

→ $\Delta E = 5.25 \times 1.986\ cal/mol \cdot K \times 300K$

→ $\Delta E = 3.13\ kcal/mol$, which is a very reasonable value.

A further question is why the nonradiative decay rate (1.67 x 10^{11} s^{-1}) is so fast in **3-HTC-DiCN**? The answer is likely to be the rotational motions along the single bonds in the molecule.

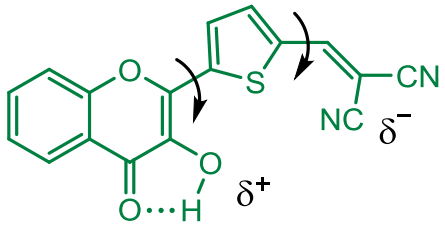

3-HTCA - Data taken from the absorption and excitation spectra (Fig. 3 & S5):

Wavelength (nm)	Relative Absorbance	Relative Emission Intensity in the Excitation Spectrum Monitored at	
		Normal Form (450 nm)	Tautomer Form (600 nm)
300	0.21	0.11	0.28
350	0.58	0.43	0.63
400	0.71	0.83	0.70

Using the data obtained at 350 and 400 nm:

For 350 nm, β = 0.58

400 nm, α = 0.71

$\rightarrow \frac{\beta}{\alpha} = \frac{0.58}{0.71} = 0.817$

For 350 nm, $I_{N(\beta)} = 0.43$ and $I_{T(\beta)} = 0.63$

400 nm, $I_{N(\alpha)} = 0.83$ and $I_{T(\alpha)} = 0.70$

$\rightarrow \frac{I_{N(\beta)}}{I_{N(\alpha)}} = \frac{0.43}{0.83} = 0.518$ and $\frac{I_{T(\beta)}}{I_{T(\alpha)}} = \frac{0.63}{0.70} = 0.900$

Plug the values into eq. 1

$\rightarrow 0.518 = 0.817(1 - y) \quad \rightarrow y = 0.366 = 36.6\%$

Then by using eq. 2

$\rightarrow 0.900 = 0.518 + 0.817 \times \frac{0.366}{x} \quad \rightarrow x = 0.783 = 78.3\%$

Using the data obtained at 300 and 400 nm:

For 300 nm, β = 0.21

400 nm, α = 0.71

$\rightarrow \frac{\beta}{\alpha} = \frac{0.21}{0.71} = 0.296$

For 300 nm, $I_{N(\beta)} = 0.11$ and $I_{T(\beta)} = 0.28$

400 nm, $I_{N(\alpha)} = 0.83$ and $I_{T(\alpha)} = 0.70$

$\rightarrow \frac{I_{N(\beta)}}{I_{N(\alpha)}} = \frac{0.11}{0.83} = 0.133$ and $\frac{I_{T(\beta)}}{I_{T(\alpha)}} = \frac{1.28}{0.70} = 0.400$

Plug the values into eq. 1

$\rightarrow 0.133 = 0.296(1 - y) \quad \rightarrow y = 0.551 = 55.1\%$

Then by using eq. 2

$\rightarrow 0.400 = 0.133 + 0.296 \times \frac{0.551}{x} \quad \rightarrow x = 0.611 = 61.1\%$

Now, the picture for **3-HTCA** is

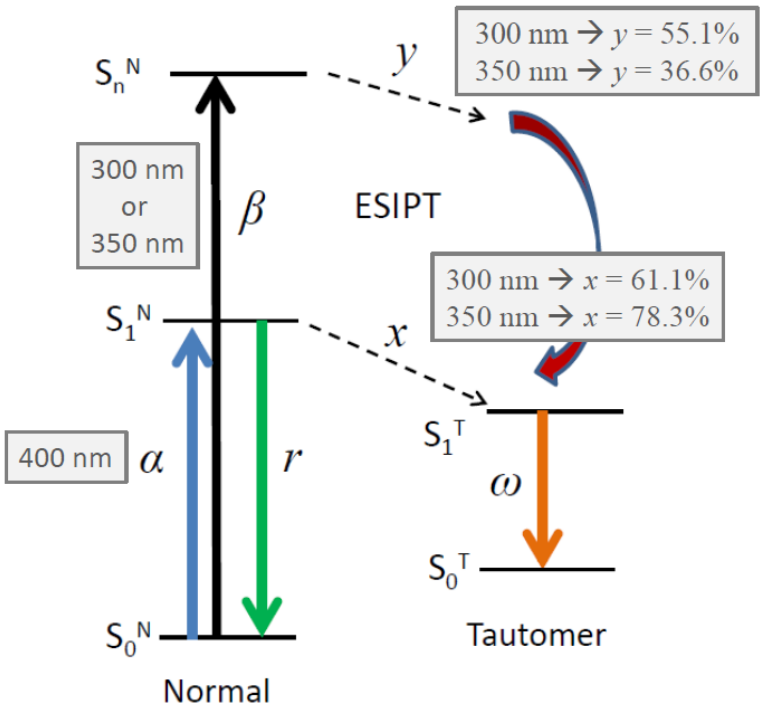

3-HTCA

The tautomer emission quantum yield (Φ_{em}) can be written as

$$\Phi_{em} = y\omega + (1 - y)x\omega$$

From Table 1, when **3-HTCA** is excited at 300 nm, the tautomer emission quantum yield (Φ_{em}) is 0.32.

$$\rightarrow 0.32 = 55.1\% \times \omega + (1 - 55.1\%) \times 61.1\% \times \omega$$

$$\rightarrow \omega = 0.39$$

This emission quantum efficiency of **3-HTCA** is higher than that of **3-HTC-DiCN** (ω = 0.18) and the observed excited-state tautomer lifetime for **3-HTCA** (6.1 ns) is also longer than **3-HTC-DiCN** (2.4 ns).

Check point:

When **3-HTCA** is excited at 350 nm, the tautomer emission quantum yield can be estimated using the equation and the ω value obtained above:

$$\Phi_{em} = y\omega + (1 - y)x\omega$$

$$\rightarrow \Phi_{em} = 36.6\% \times 0.39 + (1 - 36.6\%) \times 78.3\% \times 0.39$$

$$= 0.34$$

From Table 1, when **3-HTCA** is excited at 350 nm, the tautomer emission quantum yield (Φ_{em}) is 0.31 which is not far off from the estimated value.